ACS APPLIED MATERIALS & INTERFACES

Research Article

www.acsami.org

Transparency, Gas Barrier, and Moisture Resistance of Large-Aspect-Ratio Vermiculite Nanobrick Wall Thin Films

Morgan A. Priolo,* Kevin M. Holder,† Stephen M. Greenlee, and Jaime C. Grunlan*

Department of Mechanical Engineering, Texas A&M University, College Station, Texas 77843-3123, United States

Supporting Information

ABSTRACT: The ability to incorporate large-aspect-ratio vermiculite (VMT) clay into thin films fabricated using the layer-by-layer assembly techinique is reported for the first time. Thin films of branched polyethylenimine (PEI) and VMT were analyzed for their growth rate, clay composition, transparency, and gas barrier behavior. These films consist of >96 wt % clay, are >95% transparent, and, because of their nanobrick wall structure, exhibit super gas barrier behavior at thicknesses of <165 nm. When coupled with flexibility, the optical clarity and super barrier that these coatings can impart make them superb candidates for a variety of packaging applications.

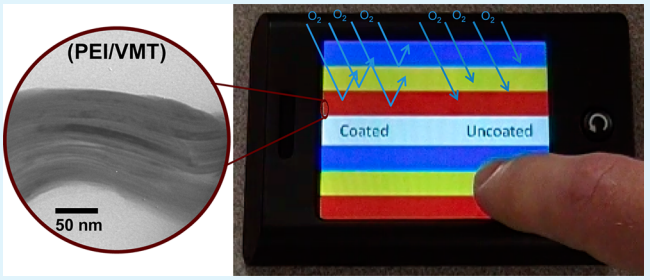

KEYWORDS: *layer-by-layer assembly, transmission electron microscopy, thin films, oxygen barrier, clays, composites*

INTRODUCTION

Current flexible display architectures, such as those used for flexible organic light-emitting diodes (FOLEDs), require a transparent barrier layer that prevents oxygen gas ingress into the device's active components. These devices require an oxygen transmission rate (OTR) below 10^{-5} $cm^3/(m^2$ day atm) to achieve sufficient performance requirements (i.e., tens of thousands of hours of operation) in ambient environments.[1,2] Similar layers with very low permeation rates to atmospheric gases are also key components for a variety of packaging applications, including food and pharmaceuticals.[3,4] Commonly used metallized plastics have sufficiently low permeation rates for most applications, but lose their utility when product visibility is desired, as in food packaging, or even a requirement, in the case of FOLEDs. A heavily investigated alternative to the metallization of plastics is the deposition of thin metal-oxide layers via vacuum-based processes, such as physical vapor deposition or plasma-enhanced chemical vapor deposition. These inorganic barrier layers exhibit very low OTR at thicknesses as low as 100 nm.[5] Despite exhibiting impressive barrier, low adhesion strength to plastics and inherent brittleness, because they are continuous ceramic sheets, make these films prone to cracking and loss of barrier performance.[6] Layering these ceramic nanocoatings with ultraviolet (UV)-curable polymer has been shown to reduce permeability; however, these multilayered coatings require very complex fabrication techniques that significantly increase cost.[7]

Clay-filled polymer composites, where individual or stacks of clay platelets are randomly dispersed in bulk polymer, offer an alternative to deposited layers on a plastic substrate. Clay nanoplatelets can be thought of as impermeable barrier particles that extend a penetrating gas molecule's travel due to their creation of a highly tortuous path. The tortuous pathway concept is the key to gas barrier performance of the polymer/clay composites.[8−10] In contrast to fully inorganic coatings, polymer/clay nanocomposites generally maintain desirable mechanical properties. Unfortunately, these composites typically suffer from clay aggregation and random platelet alignment, yielding poor transparency and relatively high gas permeation rates.[11−13] Recent one-pot mixtures of clay in polymers have led to significant improvements in platelet alignment, but they still exhibit haziness, have relatively high OTR values, and are orders of magnitude thicker than ceramic nanocoatings.[14,15]

A recent review of the clay-based nanocomposite landscape stated that the key to success for polymer/clay nanocomposites is the ability to incorporate uniformly dispersed, highly exfoliated, individual clay platelets in a polymer matrix.[16] The vast literature on this topic further suggests that finding a balance between flexibility, transparency, and barrier is vital to the successful encapsulation of flexible electronic devices.[3] Layer-by-layer (LbL) assembly is a relatively inexpensive water-based coating technique that utilizes the natural complexation of oppositely charged (or otherwise functionalized) species onto a surface.[17−19] The sequential exposure of a substrate to alternating cationic and anionic mixtures yields nanometer-scale buildup of multilayered, multifunctional thin films, where these mixtures often contain nanoparticles.[20−23] LbL deposition produces composites of highly aligned and exfoliated clay layers in a polymer matrix that remain transparent, are flexible,

Received: July 23, 2012
Accepted: September 27, 2012
Published: September 27, 2012

   dx.doi.org/10.1021/am3014289 | ACS Appl. Mater. Interfaces 2012, 4, 5529−5533

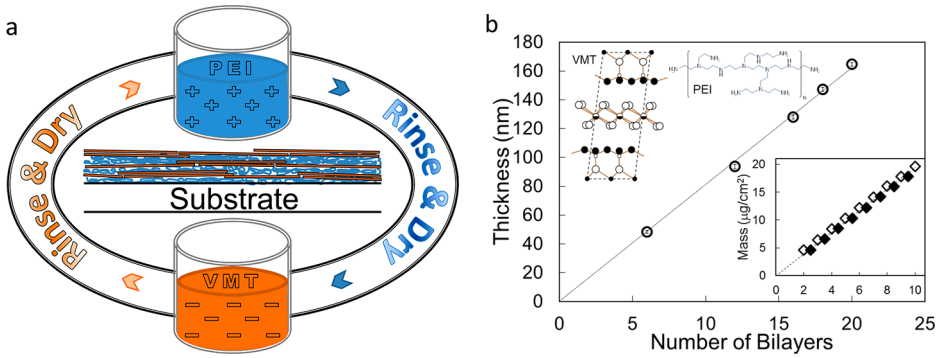

Figure 1. (a) Schematic of layer-by-layer (LbL) assembly with cationic polyethylenimine (PEI) and anionic vermiculite (VMT) clay and a cross-sectional illustration of the resultant thin film. (b) Thickness as a function of the number of PEI/VMT bilayers (BLs) deposited. The inset shows mass deposition as a function of the number of BLs deposited, with half bilayers representing PEI deposition. VMT structure legend: (•) Mg, Fe, Al; (○) O_1; ∘ Si, Al; (●) $O_{2,3}$; and (◒) Mg.[33]

and exhibit super gas barrier properties (OTR < 0.005 $cm^3/(m^2$ day atm).[24−27]

The impressive gas barrier that is reported is believed to be due to a highly aligned, nanobrick wall structure that creates extreme tortuosity for gas molecule diffusion. This type of tortuous pathway was previously modeled, resulting in a mathematical representation of relative permeability:

$$\frac{P_o}{P} = 1 + \mu\alpha^2\left(\frac{\phi^2}{1-\phi}\right) \quad (1)$$

where P_o is the polymer matrix permeability, P the composite permeability, μ a filler geometric factor, α the filler aspect ratio (defined as $(l/2)/d$), and ϕ the volume fraction of filler.[28] This model predicts that larger-aspect-ratio fillers will improve the barrier of polymer nanocomposites, with the relative permeability (P_o/P) scaling with the square of α (see eq 1). The present study demonstrates the first ever LbL assembly of cationic, branched polyethylenimine (PEI) and anionic, large-aspect-ratio vermiculite clay (VMT), which results in films that exhibit unprecedented optical clarity and super gas barrier when deposited on poly(ethylene terphthalate) (PET) film.

EXPERIMENTAL SECTION

Thin Film Materials. Specialty Vermiculite Corp. (Cambridge, MA) supplied the natural vermiculite (VMT) (Microlite 963++) clay dispersion. Branched polyethylenimine (PEI) (molecular weight of M_w = 25 000 g/mol, number-average molecular weight of M_n = 10,000 g/mol) was purchased from Sigma−Aldrich (Milwaukee, WI). Aqueous, 0.1 wt % PEI solutions were prepared using 18.2 MΩ deionized water and rolling for 24 h. Prior to deposition, the pH of each PEI solution was altered to 10, using 1 M HCl. Aqueous suspensions of VMT (2 wt % in deionized water) were prepared for 48 h before use by rolling for 24 h and allowing for sedimentation of insoluble fractions for the remaining 24 h. The unaltered supernatant was used and measured to be pH 7.5, 2 wt % VMT, and have an average effective diameter of 1.1 μm.

Substrates. Single-side-polished, silicon wafers, purchased from University Wafer (South Boston, MA), were used as substrates to monitor film growth via ellipsometry. One-millimeter-thick (1-mm-thick), fused quartz slides, purchased from Structure Probe, Inc. (West Chester, PA), were used as substrates to monitor light transmission via ultraviolet−visible light (UV-vis) spectrometry. Silicon wafers, cut to ∼4 in. × ∼1 in. strips, and ∼3 in. × ∼1 in. quartz slides, were cleaned with piranha solution for 30 min, rinsed with deionized water, acetone, and water again, and dried with filtered air prior to deposition.[29] ***Caution!*** *Piranha solution reacts violently with organic materials and should be handled with extreme care.* Polished Ti/Au crystals with a resonance frequency of 5 MHz, purchased from Maxtek, Inc. (Cypress, CA), were used as substrates to monitor mass deposition via quartz crystal microbalance (QCM). QCM crystals were plasma cleaned in a PDC-32G plasma cleaner from Harrick Plasma (Ithaca, NY) for 5 min at 10.5 W prior to deposition. Melinex ST505 poly(ethylene terphthalate) (PET) film 179 μm thick, produced by Dupont−Teijin Films and purchased from Tekra (New Berlin, WI), was used as the substrate for OTR testing and TEM images. PET was rinsed with deionized water, methanol, water again, dried with filtered air and finally corona treated using a BD-20C Corona Treater (Electro-Technic Products, Inc., Chicago, IL) prior to deposition.

Thin Film Deposition. Treated substrates were dipped in the PEI solution for 5 min, rinsed in a stream of deionized water, and dried in a stream of filtered air. This procedure was followed by an identical dipping, rinsing and drying procedure in the VMT suspension. After this initial bilayer (BL) was deposited, the same procedure was followed with 5-s PEI and 1-min VMT dip times for each subsequent layer until the desired number of layers were deposited. It was previously discovered that polymers could be deposited within seconds rather than minutes to yield equivalent assemblies from a barrier perspective.[30] All thin films were prepared using previously described home-built robotic dipping systems.[31,32] Films created for OTR testing were placed in an oven at 70 °C for 15 min immediately following deposition.

Characterization Techniques. Film thickness was measured (on silicon wafers) using an alpha-SE Ellipsometer (J.A. Woollam Co., Inc., Lincoln, NE). Mass deposition was measured (on Ti/Au crystals) using a Research Quartz Crystal Microbalance (Maxtek, Inc., Cypress, CA). Film absorbance was measured (on quartz glass slides) using a USB2000 UV-vis spectrometer (Ocean Optics, Dunedin, FL). A thin-film cross section was imaged using a transmission electron microscopy (TEM) system (Model 1200 EX, JEOL, Peabody, MA) at an accelerating voltage of 100 kV and calibrated magnifications. A 12-BL thin film was deposited on PET, coated with carbon, and embedded in epoxy prior to sectioning. Thin sections (∼100 nm thick) were floated onto water and picked up using carbon-stabilized, Formvar-coated 150-mesh nickel grids (Electron Microscopy Sciences, Hatfield, PA) in preparation for imaging. OTR and WVTR was measured (on 179-μm-thick PET), and performed by MOCON (Minneapolis, MN), using an Oxtran 2/21 ML oxygen permeability instrument (in accordance with ASTM Standard D-3985) at 23 °C and at 0% and 100% RH and a Permatran-W 3/33 water vapor permeability instrument (in accordance with ASTM Standard F-1249) at 23 °C and 100% RH. VMT particle size was determined using a ZetaPALS system (Zeta potential analyzer utilizing Phase Analysis Light Scattering) from Brookhaven Instruments Corporation (Holtsville, NY).

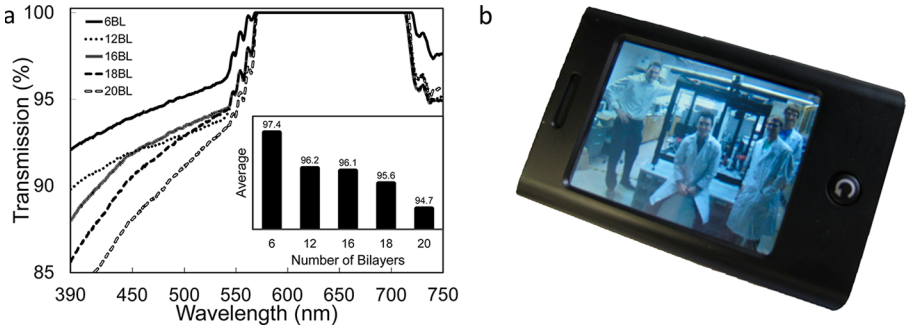

Figure 2. (a) Visible light transmission as a function of wavelength for PEI/VMT films deposited onto quartz glass. Inset shows average visible light transmission as a function of bilayers deposited. (b) An image of a half-coated media player screen is shown to highlight transparency and the utility of this technology.

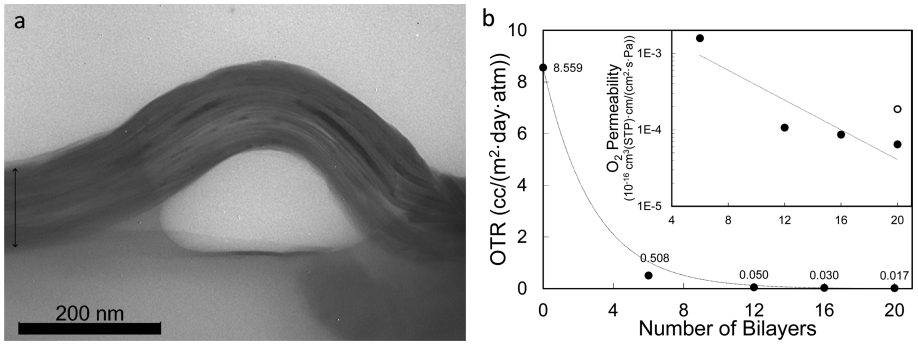

Figure 3. (a) TEM image of 12 PEI/VMT bilayers deposited onto PET film. The arrow spans the LbL film thickness. (b) Oxygen transmission rate and oxygen permeability as function of PEI/VMT bilayers (filled points) and a 20-BL PEI/MMT film[27] (unfilled point) deposited onto PET.

RESULTS AND DISCUSSION

Thin Film Growth, Composition, and Optical Clarity. Bilayers were deposited, from 0.1 wt % solutions of pH 10 PEI and 2 wt % suspensions of VMT (illustrated in Figure 1a), onto a silicon wafer to monitor film growth as a function of layers deposited, as shown in Figure 1b. Film growth is shown to increase linearly as a function of the numbers of BLs deposited, with a growth rate of ∼8 nm per BL, suggesting that all vermiculite deposition is oriented parallel to the substrate. Any significant misorientation of platelets would result in film thickness values on the order of hundreds of nanometers after only a few layers, because of the large size of individual VMT platelets (average effective diameter of ∼1.1 μm). This growth rate is greater than that shown for films deposited with the same concentration of MMT platelets, where it was proposed that the use of clay suspensions at 2 wt % led to the deposition of a very tightly packed, two-dimensional (2-D) structure and a higher possibility of multiple platelets deposited per cycle.[21] VMT platelets have a larger surface area than MMT, so it is not surprising that they have less complete exfoliation that increases the number of platelets (and thickness) deposited in each BL. Mass deposited per layer exhibits a similar linear growth trend as shown for film thickness, as shown in the inset of Figure 1b, and reveals incredibly high clay concentration at 96.6 wt %. These data support the idea of multiplatelet deposition per layer and represent the highest clay concentration ever reported for a dense polymer nanocomposite ($\rho \approx 2.4$ g/cm^3). With a thickness per BL of ∼8 nm, these stacks of platelets could total no more than four or five in each layer, which is excellent exfoliation for platelets with an α value of >1000.

UV−vis spectroscopy (Figure 2a) reveals that, even at such high clay concentrations, these films exhibit excellent transparency throughout the visible light spectrum (390−750 nm). Twenty-bilayer (20-BL) films achieve visible light transparency of >94.7% (shown as the average visible light transmission in the inset of Figure 2a), providing further evidence that clay deposition occurs in a highly oriented and exfoliated manor. Even a modest lack of clay orientation, or significant platelet stacking, with each layer deposited would have compounding effects on light transmission, exponentially decreasing transparency as a function of layers deposited, which is not exhibited here. Figure 2b shows a 20-BL coating deposited directly onto the surface of a touchscreen media player to highlight the transparency and utility of these films as an encapsulation layer for electronic displays. The coating was applied using the traditional LbL dipping process and the almost-imperceptible line running across the center of the screen is the top of the coating. The uncoated portion of the screen shows minimal differences in display emission when compared to the coated portion, with little discernible difference when viewed at varying angles (see the Supporting Information). This transparency is achieved only when clay platelets deposit in the film in a highly exfoliated state, where the thickness of individual platelets is too small to interact with visible light transmission. Also, the deposition of this nanocoating directly onto the touchscreen's surface did no harm to the touch functionality (see the Supporting Information).

Thin Film Nanostructure and Oxygen Permeability. The exfoliation state of VMT in these films is clearly observed in the cross-sectional TEM image of a 12-BL film deposited onto PET, shown in Figure 3a. Individually deposited vermiculite clay platelets can be seen in this image as dark, wavy horizontal lines, revealing the typical nanobrick wall structure exhibited by polymer/clay LbL films.[25,26] The highly aligned structure seen

in this micrograph also confirms earlier suggestions that every platelet deposited in the film lays flat, with its largest dimension parallel to the substrate. These incredibly high levels of clay loading and exfoliation are only achievable by the self-assembling, self-terminating nature of the LbL assembly process.

Figure 3b reveals that the OTR of these assemblies decreases exponentially as a function of bilayers deposited onto PET film. A 6-BL film, only 48 nm thick, lowers the OTR by more than an order of magnitude, from 8.6 $cm^3/(m^2$ day atm) for bare PET to 0.5 $cm^3/(m^2$ day atm), making it useful for food packaging and LED/LCD panel or photovoltaic device encapsulation.[34] After 20 BL are deposited onto PET, this system exhibits super gas barrier properties, with an OTR of 0.017 $cm^3/(m^2$ day atm). The inset in Figure 3b reveals that the oxygen permeability of these films also decreases exponentially as a function of bilayers deposited, which is a phenomenon unique to these LbL thin films.[25,27] While film thickness is increased by a factor of 3.4, from 6 BLs to 20 BLs, thin film permeability decreases by a factor of 25. More impressive is the OTR disparity of these same films, where OTR decreases by more than an order of magnitude, from 6 BLs to 20 BLs.

The super oxygen barrier of these thin film assemblies (summarized in Table 1) is believed to be due to the existence

Table 1. Volume Fraction of Clay, Oxygen Transmission Rates, and BIF of Films Deposited on 179 μm PET

thin film assembly	volume fraction clay (ϕ)	OTR (cm^3/m^2 day atm)	oxygen permeability ($\times 10^{-16}$ cm^3(STP) cm/(cm^2 s Pa)) coating[a]	oxygen permeability ($\times 10^{-16}$ cm^3(STP) cm/(cm^2 s Pa)) total	BIF[b]
179-μm-thick PET		8.559		17.50	
$(PEI/VMT)_{20}$	0.92	0.017	0.000064	0.035	500
$(PEI/MMT)_{20}$[c]	0.83	0.078	0.00019	0.16	110

[a]Coating permeability was decoupled from the total using a previously described method.[35] [b]BIF = P_S/P_T, where P_S is the uncoated PET permeability and P_T is the coated permeability. [c]Data are previously published results.[27]

of a nanobrick wall structure, revealed in Figure 3a, which creates a tortuous pathway for permeating gas molecules. While diffusing through the thin film assembly, gas molecules must travel around individually deposited (or stacks of just a few) VMT platelets, which significantly extends the diffusion length traveled. This larger residence time of a permeating molecule in the film's thickness yields a lower rate of gas permeation, as modeled by Cussler.[28] When compared to a previously reported thin film of PEI/MMT, the films in this study utilize vermiculite clay that has an aspect ratio that is an order of magnitude larger than MMT and is shown to deposit more clay in the thin film (92 vol % VMT, compared to 83 vol % MMT), as shown in Table 1. The volume fraction of clay deposited was calculated by converting the measured mass fractions, shown in the inset of Figure 1b, to volumetric values, using the reported densities of VMT (2.5 g/cm^3) and PEI (1.03 g/cm^3). This combination of larger aspect ratio and higher clay concentration results in a 20-BL VMT-based film to exhibit an OTR that is a factor of 3 lower than the same film made with MMT. In addition, as seen in Table 1, this simple alteration of clay platelet choice is capable of improving the barrier improvement factor (BIF, defined as the uncoated PET permeability divided by the coated permeability) by a factor of 5, where 20 BLs of PEI/VMT yield a BIF of 500, as compared to BIF = 110 for films made with MMT deposited on 179-μm-thick PET.

Humidity Resistance and Moisture Barrier. The OTR values in Table 1 were measured under dry conditions (0% RH), but it is well-known that LbL film properties degrade under elevated humidity.[24,26,36] Oxygen barrier performance under humid conditions was evaluated by testing the OTR of a 20-BL film deposited onto PET at 100% RH. Figure 4 shows

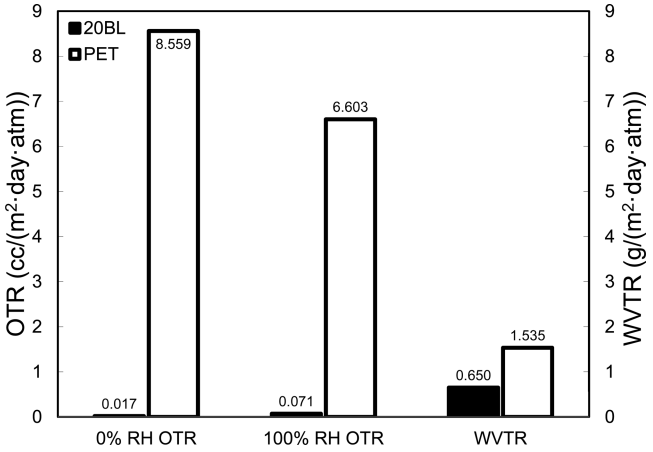

Figure 4. Oxygen transmission rate (OTR) and water vapor transmission rate (WVTR) values of 179-μm-thick PET film and 20-BL VMT-based assemblies on PET.

that the OTR values of the 20-BL film increases as a function of relative humidity (RH); however, this increase is much less than that reported previously for MMT-based thin films.[24,26] The 20-BL coating exhibits a decrease in barrier by a factor of 4 when exposed to 100% RH. This is in stark contrast to the polymer/clay coatings previously reported, which suffered orders-of-magnitude increases in OTR when exposed to similar humidity levels.

LbL gas barrier films have also been mostly tested for their low permeability to oxygen gas, with water vapor transmission rate (WVTR) values generally left untested. This 20-BL coating was deposited on PET, which has a WVTR value of ~1.5 $g/(m^2$ day atm), and exhibited a WVTR improvement of 57% (see Figure 4). This large improvement in water vapor barrier is impressive for films created from dilute, aqueous mixtures and is believed to be due to the tightly packed, highly aligned nanobrick wall structure (Figure 3a) comprised of 96.6 wt % (92 vol %) VMT. These factors lead to films that are less sensitive to humidity and impart a water vapor barrier improvement of more than a factor of 2 on 179-μm-thick PET, at a thickness of <165 nm.

CONCLUSIONS

In conclusion, vermiculite clay was deposited successfully, for the first time in a layer-by-layer (LbL) film, alongside polyethylenimine (PEI). Film growth measured on a silicon wafer demonstrates a linear growth rate of ~8 nm per bilayer, while deposition onto quartz glass sides reveals that a 20-bilayer (20-BL) film remains 95% transparent with 96.6 wt % (92 vol %) clay. When deposited onto 179-μm-thick poly(ethylene

terphthalate) (PET) film, this 20-BL nanocoating exhibits an oxygen transmission rate (OTR) value that is an order of magnitude less than that for a similar coating produced with MMT clay, yielding a barrier improvement factor of 500. These films also exhibit a less humidity-sensitive oxygen barrier and improve the water vapor transmission rate (WVTR) of PET by over 50%. At a thickness of only 164 nm, this completely transparent and highly flexible film is among the best polymer/clay nanocomposites ever reported for gas barrier, and it represents an inexpensive, relatively simple alternative to inorganic layers for a variety of packaging applications.

■ ASSOCIATED CONTENT

Supporting Information

Video highlighting the utility and transparency of a PEI/VMT coating on a touchscreen media player. This material is available free of charge via the Internet at http://pubs.acs.org.

■ AUTHOR INFORMATION

Corresponding Author

* Tel.: (979) 845-3027 (J.G.), (979) 845-1918 (M.P.). Fax: (979) 845-3081. E-mail: jgrunlan@tamu.edu (J.G.); mapriolo25@gmail.com (M.P.).

Present Address

[†]Department of Chemistry, Texas A&M University, College Station, TX 77843−3012, USA.

Author Contributions

The manuscript was written through contributions of all authors. All authors have given approval of the final version of the manuscript.

Notes

The authors declare no competing financial interest.

■ ACKNOWLEDGMENTS

The authors would like to thank The Dow Chemical Company and the Texas Engineering Experiment Station (TEES) for financial support of this research.

■ REFERENCES

(1) Burrows, P. E.; Graff, G. L.; Gross, M. E.; Martin, P. M.; Shi, M. K.; Hall, M.; Mast, E.; Bonham, C.; Bennett, W.; Sullivan, M. B. *Displays* **2001**, *22*, 65−69.

(2) Kumar, R. S.; Auch, M.; Ou, E.; Ewald, G.; Jin, C. S. *Thin Solid Films* **2002**, *417*, 120−126.

(3) Graff, G. L.; Burrows, P. E.; Williford, R. E.; Praino, R. F. In *Flexible Flat Panel Displays*; Crawford, G. P., Ed.; John Wiley & Sons, Ltd.: New York, 2005; pp 57−77.

(4) Jagadish, R. S.; Raj, B.; Asha, M. R. *J. Appl. Polym. Sci.* **2009**, *113*, 3732−3741.

(5) Inagaki, N.; Tasaka, S.; Hiramatsu, H. *J. Appl. Polym. Sci.* **1999**, *71*, 2091−2100.

(6) Leterrier, Y. *Prog Mater. Sci.* **2003**, *48*, 1−55.

(7) Affinito, J. D.; Gross, M. E.; Coronado, C. A.; Graff, G. L.; Greenwell, E. N.; Martin, P. M. *Thin Solid Films* **1996**, *290*, 63−67.

(8) Paul, D. R.; Robeson, L. M. *Polymer* **2008**, *49*, 3187−3204.

(9) Choudalakis, G.; Gotsis, A. D. *Eur. Polym. J.* **2009**, *45*, 967−984.

(10) Duncan, T. V. *J. Colloid Interface Sci.* **2011**, *363*, 1−24.

(11) Grunlan, J. C.; Grigorian, A.; Hamilton, C. B.; Mehrabi, A. R. *J. Appl. Polym. Sci.* **2004**, *93*, 1102−1109.

(12) Kumar, S. A.; He, Y. L.; Ding, Y. M.; Le, Y.; Kumaran, M. G.; Thomas, S. *Ind. Eng. Chem. Res.* **2008**, *47*, 4898−4904.

(13) Triantafyllidis, K. S.; LeBaron, P. C.; Park, I.; Pinnavaia, T. J. *Chem. Mater.* **2006**, *18*, 4393−4398.

(14) Ebina, T.; Mizukami, F. *Adv. Mater.* **2007**, *19*, 2450−2453.

(15) Walther, A.; Bjurhager, I.; Malho, J. M.; Pere, J.; Ruokolainen, J.; Berglund, L. A.; Ikkala, O. *Nano Lett.* **2010**, *10*, 2742−2748.

(16) Gao, F. *Mater. Today* **2004**, *7*, 50−55.

(17) Decher, G.; Hong, J. D.; Schmitt, J. *Thin Solid Films* **1992**, *210*, 831−835.

(18) Hammond, P. T. *Adv. Mater.* **2004**, *16*, 1271−1293.

(19) Ariga, K.; Hill, J. P.; Ji, Q. M. *Phys. Chem. Chem. Phys.* **2007**, *9*, 2319−2340.

(20) Kleinfeld, E. R.; Ferguson, G. S. *Science* **1994**, *265*, 370−373.

(21) Alazemi, M.; Dutta, I.; Wang, F.; Blunk, R. H.; Angelopoulos, A. P. *Adv. Funct. Mater.* **2009**, *19*, 1118−1129.

(22) Feller, J. F.; Lu, J.; Zhang, K.; Kumar, B.; Castro, M.; Gatt, N.; Choi, H. J. *J. Mater. Chem.* **2011**, *21*, 4142−4149.

(23) Ratanatawanate, C.; Perez, M.; Gnade, B. E.; Balkus, K. J. *Mater. Lett.* **2012**, *66*, 242−245.

(24) Jang, W. S.; Rawson, I.; Grunlan, J. C. *Thin Solid Films* **2008**, *516*, 4819−4825.

(25) Priolo, M. A.; Gamboa, D.; Grunlan, J. C. *ACS Appl. Mater. Interfaces* **2010**, *2*, 312−320.

(26) Priolo, M. A.; Gamboa, D.; Holder, K. M.; Grunlan, J. C. *Nano Lett.* **2010**, *10*, 4970−4974.

(27) Priolo, M. A.; Holder, K. M.; Gamboa, D.; Grunlan, J. C. *Langmuir* **2011**, *27*, 12106−12114.

(28) Cussler, E. L.; Hughes, S. E.; Ward, W. J.; Aris, R. *J. Membr. Sci.* **1988**, *38*, 161−174.

(29) Geddes, N. J.; Paschinger, E. M.; Furlong, D. N.; Caruso, F.; Hoffmann, C. L.; Rabolt, J. F. *Thin Solid Films* **1995**, *260*, 192−199.

(30) Yang, Y. H.; Malek, F. A.; Grunlan, J. C. *Ind. Eng. Chem. Res.* **2010**, *49*, 8501−8509.

(31) Jang, W. S.; Grunlan, J. C. *Rev. Sci. Instrum.* **2005**, *76*, 103904.

(32) Gamboa, D.; Priolo, M. A.; Ham, A.; Grunlan, J. C. *Rev. Sci. Instrum.* **2010**, *81*, 036103.

(33) Mathieson, A. M. *Am. Mineral.* **1958**, *43*, 216−227.

(34) Charton, C.; Schiller, N.; Fahland, M.; Hollander, A.; Wedel, A.; Noller, K. *Thin Solid Films* **2006**, *502*, 99−103.

(35) Roberts, A. P.; Henry, B. M.; Sutton, A. P.; Grovenor, C. R. M.; Briggs, G. A. D.; Miyamoto, T.; Kano, A.; Tsukahara, Y.; Yanaka, M. *J. Membr. Sci.* **2002**, *208*, 75−88.

(36) Nolte, A. J.; Treat, N. D.; Cohen, R. E.; Rubner, M. F. *Macromolecules* **2008**, *41*, 5793−5798.